New Measurement Algorithm for Supraharmonics based on Multiple Measurement Vectors Model and Orthogonal Matching Pursuit

Shuangyong Zhuang, Wei Zhao, Ren Wang, Qing Wang, Senior Member, IEEE, and Songling Huang, Senior Member, IEEE

***Abstract*—There are many cases of electromagnetic interference caused by supraharmonics emitted by power electronic equipment. However, there is currently no effective method for measuring supraharmonics. This paper proposes a new supraharmonics high-resolution measurement algorithm based on a multiple measurement vectors compressive sensing model and an orthogonal matching pursuit recovery algorithm. Firstly, the algorithm, based on a spectrum array of multiple DFT coefficient vectors and a Dirichlet kernel matrix, constructs a multiple measurement vectors compressive sensing model by introducing an interpolation factor. Then, by using the jointly sparse property of high-resolution spectrum array, the multiple measurement vectors compressive sensing model is converted into a single measurement vector compressive sensing model. Thirdly, by using an orthogonal matching pursuit recovery algorithm, we solve the support set of the high-resolution spectrum array. Finally, we use least squares to realize the high-resolution analysis of supraharmonics spectrum array simultaneously. Simulation results and verification of the measured data show that the algorithm proposed in this paper can save the calculation time by 100 times, can improve the frequency resolution by an order-of-magnitude without increasing the observation time, and can compute the frequency and magnitude of supraharmonics accurately. By combing the algorithm with 3-D display method, we can see the dynamic time-varying characteristics of supraharmonics clearly. This algorithm shows a good application prospect in measuring supraharmonics more accurately.**

***Index Terms*—Supraharmonics, Compressive sensing, Multiple measurement vectors model, Orthogonal matching pursuit.**

I. Introduction

With the popularity of new energy technologies and smart grid control technologies, more and more power electronic equipment, such as photovoltaic inverters, electric vehicle charging piles, switching power supplies, new lighting devices, home appliances and power line carrier communication equipment, are applied in the power system. While achieving energy-saving, high-efficiency, and intelligence, they also emit more and more high-frequency distortion [1] in 2 to 150 kHz into the power system, which has caused a series of new electromagnetic interference problems [2]. For example, the malfunction of automatic meter reading and inaccuracy of energy metering; the degraded copying quality of a copying machine due to the interference caused by a computer number control machine nearby; damage to the filter capacitor of the power supply inverter in the automotive punching workshop, so the punching machine cannot work properly; a precision instrument sharing the power socket with the CNC machine is burned[3]; the resonance between the motor tester circuit and the breaker circuit causes abnormal noise, et.al.. In 2013, at an IEEE International Conference on Power and Energy, Emanuel first defined the high-frequency distortion in 2 to 150 kHz as supraharmonics [4]. Subsequently, this concept was gradually accepted by the industry. In the latest standard IEC 61000-2-2, supraharmonics are clearly divided into intentional emission and unintentional emission. The so-called intentional emission refers to the power line carrier communication signal, and the unintentional emission refers to conducted emission that is not intended for communication purpose. Electromagnetic interference is mainly caused by unintentional emission. In 2010, 2013 and 2015, the European Committee for Electrotechnical Standardization (CENELEC) successively released three research reports on electromagnetic interference between electrical equipment and systems in the frequency range below 150 kHz [5]. In 2017, the International Conference on Electricity Distribution (CIRED) specially set up a special report for supraharmonics [6]. Undoubtedly, supraharmonics has caused a great deal of attention from universities, research institutions and relevant international standardization organizations.

In the newly revised standard IEC 61000-4-30, annex C, three measurement methods for supraharmonics are recommended. One method is to extend the gapless clustering method in IEC 61000-4-7, annex B, from the present 9 kHz limit up to the 150 kHz limit. A second method under consideration is the newly proposed 32 equal-width segments measurement method. A third method is the method of CISPR 16-1-2. Due to the different measurement principles of the three measurement methods, the measurement results obtained by them must be quite different [7].

The spectral leakage of the gapless clustering measurement method is severe. The basic principle of the 32 equal-width segments measurement method is to extract 32 sets of 0.5 ms of data block from 200 ms of measured signal, and perform a DFT transform separately to obtain 32 sets of spectrums with 2 kHz frequency resolution, and the maximum, minimum and average values of each spectral line are counted. Since this method uses only about 8% of the measured data, the number of calculations can be significantly reduced and it is most likely to become the

Shuangyong Zhuang, Wei Zhao, Ren Wang, and Songling Huang are with the State Key Lab. Of Power System, Department of Electrical Engineering, Tsinghua University, Beijing, 100084, China (e-mail: zhaowei@mail.tsinghua.edu.cn).

Qing Wang is with the Department of Engineering, Durham University, Durham, UK.

standard supraharmonics measurement method. However, this method has some disadvantages, e.g. the mutual limitation between observation time and frequency resolution, and large frequency resolution, means that the components of supraharmonics cannot be positioned precisely. At the same time, because of the measurement with gap, some parts of the signal under test will be undetected because it is always in a gap [8]. Furthermore, since the supraharmonics has a dynamic time-varying characteristic, that is, the frequency, amplitude and phase of the supraharmonics will change dynamically with time, this method cannot analyze the dynamic characteristics of supraharmonics.

The CISPR 16-1-2 measurement method can only measure one value each time, and the measurement time is longer, which cannot meet the real-time measurement requirements.

In order to research the propagation property, interaction mechanism, emission limits, and inhibition of supraharmonics, it is necessary to measure supraharmonics accurately. Therefore, it is a big challenge to propose an effective supraharmonics high-resolution measurement algorithm.

Spatial spectrum estimation methods such as Multiple Signal Classification (MUSIC) [9] and Estimation of Signal Parameters via Rotational Invariance Techniques (ESPRIT) [10] have been applied to harmonics and interharmonics because of their super-resolution, but at the cost of higher computational complexity. The spectrum of supraharmonics, generated by power electronics at its switching frequency and integral multiple, is sparse in the frequency domain. Therefore, this kind of signal can be analyzed by using compressive sensing (CS) [11]-[13]. [14] proposed a high-resolution harmonic analysis algorithm based on compressive sensing, which can increase the frequency resolution of traditional harmonics by an order of magnitude, but can only process one data spectrum. [15] proposed a supraharmonics high-resolution measurement method based on a single measurement vector (SMV) compressive sensing model and orthogonal matching pursuit (OMP) [16] recovery algorithm (SCS-OMP). The SCS-OMP algorithm can refine the frequency resolution from 2 kHz to 200 Hz, breaking through the limitation of Shannon's sampling theorem and overcoming the inherent limitations of mutual limitation of observation time and frequency resolution. Parameters of supraharmonics can be computed accurately and spectral leakage can be effectively inhibited.

Because of the dynamic time-varying characteristics of supraharmonics, it requires us not only to analyze supraharmonics with high-resolution, but also analyze its dynamic characteristics. Therefore, it is obviously not enough to analyze only 32 data blocks. However, the SCS-OMP algorithm can only process one supraharmonics spectrum each time. Therefore, it needs multiple iterations for 200 ms measured data, which will undoubtedly require longer time. Therefore, the algorithm does not meet the real-time requirements for supraharmonics.

In this paper, we propose a new supraharmonics high-resolution measurement algorithm based on multiple measurement vectors (MMV) [17] compressive sensing model and OMP recovery algorithm (MCS-OMP), which can realize supraharmonics high-resolution analysis of an original spectrum array (OSA) simultaneously. Each column vector corresponds to the frequency spectrum of a data block. In order to optimize the algorithm, it is noted that the high-resolution spectrum array is jointly sparse. According to [18], the original spectrum array is converted into a single eigenvector containing only supraharmonics components. Therefore, the MMV compressive sensing model is transformed into a single measurement vector (SMV) [17] compressive sensing model, and the support set is calculated using the OMP algorithm. Since the SMV compressive sensing model eliminates noise, the calculation of the support set is more stable. Finally, the supraharmonics high-resolution analysis of OSA is performed simultaneously through the least-squares method, and the calculation time can be significantly reduced. It is expected to be applied to the real-time measurement and analysis of supraharmonics.

This paper is organized as follows. The basic principles of the MCS-OMP algorithm is introduced in the next section. Section III introduces the simulation results of the supraharmonics high-resolution analysis and section IV discusses the supraharmonics high-resolution analysis of measured data. In section V, the contributions and conclusions of this paper are reviewed.

II. Principle of MCS-OMP Supraharmonics High-resolution Algorithm

A. MMV compressive sensing model

For a 200 ms power signal sampling data sequence containing supraharmonics, a digital band-pass filter is used to filter out the conventional harmonics below 2 kHz and the frequency components above 150 kHz, and then the data is uniformly divided into 400 groups of ΔT=0.5 ms small data blocks by applying a rectangular window function. Supraharmonics components contained in any small data block can be expressed as a multi-tone signal

$$x(n)=\sum_{sh}A_{sh}\cos(2\pi f_{sh}nT_{\mathrm{s}}+\theta_{sh})+w, n\in(1,N) \tag{1}$$

where A_{sh}, f_{sh}, and θ_{sh} are the amplitude, frequency and initial phase of supraharmonics, respectively. T_{s} is the sample interval, which is the reciprocal of the sample frequency f_{s}. The sequence length is $N=f_{\mathrm{s}}\Delta T$.

(1) can be expressed in Euler form.

$$x(n)=\sum_{sh}(\frac{A_{sh}}{2}e^{j[\theta_{sh}+2\pi f_{sh}nT_{\mathrm{s}}]}+\frac{A_{sh}}{2}e^{-j[\theta_{sh}+2\pi f_{sh}nT_{\mathrm{s}}]}) \tag{2}$$

The Discrete Fourier Transform (DFT) of $x(n)$ can be expressed as follows

$$\frac{2}{N}X(k)=\sum_{sh}A_{sh}e^{j\theta_{sh}}D(\frac{k}{N}-f_{sh}T_{\mathrm{s}}) \tag{3}$$

where $0\le k\le N$, the frequency resolution $\Delta f=f_{\mathrm{s}}/N$ is 2 kHz, and $D(\cdot)$ is the Dirichlet kernel matrix

$$D(\tau)=\frac{1}{N}\sum_{n=0}^{N-1}e^{-j2\pi n\tau}=\frac{\sin\pi N\tau}{N\sin\pi\tau}e^{-j\pi(N-1)\tau} \tag{4}$$

In order to improve the frequency resolution, the interpolation factor F is introduced. Therefore, the frequency resolution is refined to $\Delta' f = \Delta f / F$ and the total spectral line is $N' = NF$. Besides,

$$f_{sh} T_s \simeq \frac{r}{N'} \tag{5}$$

where r is the rth spectral line in the new frequency resolution.

The final expression is as follows

$$\frac{2}{N} X(k) \simeq \sum_{r} A_{sh} e^{j\theta_{sh}} D_N\left(\frac{k}{N} - \frac{r}{N'}\right) \tag{6}$$

where $k \in [0, N-1]$, and $r \in [0, N'-1]$

Here, we transform (6) into a SMV compressive sensing model

$$\begin{bmatrix} s_1 \\ s_2 \\ \vdots \\ s_N \end{bmatrix} \approx \begin{bmatrix} D_{11} & D_{12} & D_{13} & \cdots & D_{1N'} \\ D_{21} & D_{22} & D_{23} & \cdots & D_{2N'} \\ \vdots & \vdots & \vdots & \cdots & \vdots \\ D_{N1} & D_{N2} & D_{N3} & \cdots & D_{NN'} \end{bmatrix} \begin{bmatrix} a_1 \\ a_2 \\ a_3 \\ \vdots \\ a_{N'} \end{bmatrix} \tag{7}$$

where the element $D_{(k,r)}$ is

$$D_{(k,r)} = D\left(\frac{k}{N} - \frac{r}{N'}\right) = \frac{\sin \pi N\left(\frac{k}{N} - \frac{r}{N'}\right)}{N \sin \pi\left(\frac{k}{N} - \frac{r}{N'}\right)} e^{-j\pi(N-1)\left(\frac{k}{N} - \frac{r}{N'}\right)} \tag{8}$$

By (7), we can get a high-resolution spectrum vector from the original spectrum vector. The simplified form of (7) is as follows

$$\mathbf{s} \approx \mathbf{D}\mathbf{a} + \mathbf{w} \tag{9}$$

where $\mathbf{s}$ is the original spectrum vector, $\mathbf{D}$ is the sensing matrix, $\mathbf{a}$ is the high-resolution spectrum vector that has a K-sparsity ($K \ll N'$), $\mathbf{w}$ is the noise vector.

In order to realize the supraharmonics high-resolution analysis of M original spectrum vectors simultaneously, M original spectrum column vectors are assembled into an original spectrum array $\mathbf{S}$, and we finally construct a MMV compressive sensing model.

$$\mathbf{S} = \mathbf{D}\mathbf{A} + \mathbf{W} \tag{10}$$

where

$$\mathbf{S} = \begin{bmatrix} s_{11} & s_{12} & \cdots & s_{1M} \\ s_{21} & s_{21} & \cdots & s_{2M} \\ \vdots & \vdots & \ddots & \vdots \\ s_{N1} & s_{N1} & \cdots & s_{NM} \end{bmatrix}$$

$$\mathbf{A} = \begin{bmatrix} a_{11} & a_{12} & \cdots & a_{1M} \\ a_{21} & a_{21} & \cdots & a_{2M} \\ \vdots & \vdots & \ddots & \vdots \\ a_{N'1} & a_{N'2} & \cdots & a_{N'M} \end{bmatrix}$$

$$\mathbf{W} = \begin{bmatrix} w_{11} & w_{12} & \cdots & w_{1M} \\ w_{21} & w_{21} & \cdots & w_{2M} \\ \vdots & \vdots & \ddots & \vdots \\ w_{N1} & w_{H2} & \cdots & w_{NM} \end{bmatrix}$$

$\mathbf{S}$ is the original spectrum array, $\mathbf{D}$ is the sensing matrix, $\mathbf{A}$ is the high-resolution spectrum array, and $\mathbf{W}$ is the noise matrix. The element $s_{k,m}$ can be expressed as follows

$$s_{k,m} \simeq \sum_{r \in \Lambda} A_{sh} e^{j(\theta_{sh} + 2\pi \frac{r}{N'} i_m)} D_N\left(\frac{k}{N} - \frac{r}{N'}\right) \tag{11}$$

where i_m represents the start of the time domain signal for each data block.

B. Support set calculation for high-resolution spectrum array

1) Transformation MMV model to SMV model

If the traditional compressive sensing method is directly used to estimate the support set in the MMV model, there are two drawbacks. One is that the amount of computation is large. Second, the signal subspace and the noise subspace cannot be distinguished, which means the support set cannot be estimated accurately due to noise interference. Since the high-resolution spectrum array is jointly sparse, that is, its support set for each column is the same, it is possible to express the jointly support set of the high-resolution spectrum array by solving a SMV support set. In this way, the support set solution problem of the MMV compressive sensing model is transformed into the support set solution problem of a SMV compressive sensing model.

First, we calculate the autocorrelation matrix $\mathbf{R}_S$ of the original spectrum array $\mathbf{S}$.

$$\mathbf{R}_S = E\left[\mathbf{S}\mathbf{S}^H\right] \tag{12}$$

where the superscript H denotes transposition and complex conjugation. Replacing $\mathbf{S}$ with (10), then (12) can be transformed into

$$\begin{aligned} \mathbf{R}_S &= E\left[(\mathbf{D}\mathbf{A} + \mathbf{W})(\mathbf{D}\mathbf{A} + \mathbf{W})^H\right] \\ &= \mathbf{D}\mathbf{R}_A\mathbf{D}^H + \sigma_w^2\mathbf{I} \end{aligned} \tag{13}$$

where $\mathbf{R}_A = E\left[\mathbf{A}\mathbf{A}^H\right]$, σ_w^2 is the variance of Gaussian white noise, and $\mathbf{I}$ is the identity matrix.

The eigenvalue decomposition of $\mathbf{D}\mathbf{R}_A\mathbf{D}^H$ is

$$\mathbf{D}\mathbf{R}_A\mathbf{D}^H = \mathbf{V}_S\mathbf{\Lambda}_S\mathbf{V}_S^H \tag{14}$$

And the eigenvalue decomposition of $\mathbf{R}_S$ is

$$\mathbf{R}_S = \mathbf{V}_S\mathbf{\Lambda}\mathbf{V}_S^H \tag{15}$$

where $\mathbf{\Lambda} = \mathbf{\Lambda}_S + \sigma_w^2\mathbf{I}$. Denote the K largest eigenvalues in the diagonal matrix $\mathbf{\Lambda}_S$ as σ_1^2, σ_2^2, …, σ_K^2. The eigenvalues of $\mathbf{R}_S$ are given as follows

$$\lambda_i = \begin{cases} \sigma_i^2 + \sigma_w^2, i = 1, \cdots, K \\ \sigma_w^2, \qquad i = K+1, \cdots, N \end{cases}$$

If the signal-to-noise ratio (SNR) is large enough, σ_K^2 is significantly larger than σ_w^2. Then we call the top K largest eigenvalues of the autocorrelation matrix $\mathbf{R}_S$ as primary eigenvalues, and the other N-K smallest eigenvalues as secondary eigenvalues. The primary eigenvalues are as follows

$$\lambda_1 = \sigma_1^2 + \sigma_w^2,\ \lambda_2 = \sigma_2^2 + \sigma_w^2,\ \ldots,\ \lambda_K = \sigma_K^2 + \sigma_w^2.$$

and the secondary eigenvalues are as follows

$$\lambda_{K+1} = \lambda_{K+2} = \cdots = \lambda_N = \sigma_w^2 .$$

Correspondingly, the eigenvectors can be divided into

$$\mathbf{V}_S = [\mathbf{v}_1, \cdots, \mathbf{v}_K \,|\, \mathbf{v}_{K+1}, \cdots, \mathbf{v}_N] = [\mathbf{T}, \mathbf{G}] \tag{16}$$

where $\mathbf{T}^H \mathbf{G} = 0$. Thus, we decompose the data space into signal subspace $\mathrm{Span}(\mathbf{T}) = \mathrm{Span}[\mathbf{v}_1, \cdots, \mathbf{v}_K]$ and noise subspace $\mathrm{Span}(\mathbf{G}) = \mathrm{Span}[\mathbf{v}_{K+1}, \cdots, \mathbf{v}_N]$. Due to

$$\begin{aligned}
\mathrm{Span}(\mathbf{S}) &= \mathrm{Span}[\mathbf{s}_1, \cdots, \mathbf{s}_M] \\
&= \left\{ \mathbf{y} \in \mathbb{C}^{N\times 1} : \mathbf{y} = \sum_{i=1}^{M} x_i \mathbf{s}_i,\ x_i \in \mathbb{C} \right\} \\
&= \left\{ \mathbf{y} \in \mathbb{C}^{N\times 1} : \mathbf{y} = \mathbf{S}\mathbf{x}, \mathbf{x} \in \mathbb{C}^{M\times 1} \right\} \\
&= \left\{ \mathbf{y} \in \mathbb{C}^{N\times 1} : \mathbf{y} = \sum_{i=1}^{K} \gamma_i \mathbf{v}_i \mathbf{q}_i^H \mathbf{x}, \mathbf{x} \in \mathbb{C}^{M\times 1} \right\} \\
&= \left\{ \mathbf{y} \in \mathbb{C}^{N\times 1} : \mathbf{y} = \sum_{i=1}^{K} \mathbf{v}_i \left(\gamma_i \mathbf{q}_i^H \mathbf{x}\right), \mathbf{x} \in \mathbb{C}^{M\times 1} \right\} \\
&= \left\{ \mathbf{y} \in \mathbb{C}^{N\times 1} : \mathbf{y} = \sum_{i=1}^{K} \alpha_i \mathbf{v}_i,\ \ \alpha_i = \gamma_i \mathbf{q}_i^H \mathbf{x} \in \mathbb{C} \right\} \\
&= \mathrm{Span}[\mathbf{v}_1, \cdots, \mathbf{v}_K] \\
&= \mathrm{Span}(\mathbf{T})
\end{aligned} \tag{17}$$

Therefore, we multiply the eigenvectors matrix $\mathbf{T}$ by the column vector $\mathbf{d}_K$ composed of the square roots of the top K largest eigenvalues, to obtain eigenvalue column vector $\mathbf{v}$

$$\mathbf{v} = \mathbf{T}\mathbf{d}_K \tag{18}$$

Since the column vector $\mathbf{v}$ only retains the supraharmonics components and eliminates the noise. Finally, the MMV compressive sensing model is converted into a SMV compressive sensing model

$$\mathbf{v} = \mathbf{D}\mathbf{u} \tag{19}$$

Next, we will compute the support set $\mathbf{\Lambda}$ of support column vector $\mathbf{u}$ by using the OMP recovery algorithm.

2) Using OMP recovery algorithm to calculate support set

Since the OMP algorithm is a greedy method that implements iterative approximation by the least squares method, the residual obtained by each iteration is orthogonal to all selected column vectors, and has the advantages of fast operation speed and easy implementation. We use the OMP algorithm to calculate the support set of the constructed SMV model. The flows of the OMP algorithm are given in TABLE I.

C. Least squares method to recover high-resolution spectrum array

After recovering the support set $\mathbf{\Lambda}$ and the sub-matrix $\mathbf{D}_s$, we can recover the high-resolution spectrum array by using the least squares method.

$$\hat{\mathbf{A}} = \arg\min \|\mathbf{S} - \mathbf{D}_S \mathbf{A}\|_2 = (\mathbf{D}_S{}^H \mathbf{D}_S)^{-1} \mathbf{D}_S{}^H \mathbf{S} \tag{20}$$

where $\hat{\mathbf{A}}$ includes *M* columns of a high-resolution spectrum column vector. Each column corresponds to the phasor information of each supraharmonic at different times. The frequency, amplitude and phase matrix of the supraharmonics are obtained by

TABLE I
FLOW FOR OMP ALGORITHM

1). Initialization
1. Input eigenvalue column vector $\mathbf{v}$, sensing matrix $\mathbf{D}$, sparsity *K*, and threshold ε_{th}
2. Initialize parameters: residual $\mathbf{r}_0 = \mathbf{v}$, support set $\mathbf{\Lambda}_0 = \varnothing$, sub-matrix $\mathbf{D}_0 = []$, ant iteration time $t = 1$.
2). Iteration approximation
1. Find the index $\lambda_t = \arg\max |< \mathbf{d}_i, \mathbf{r}_{t-1} >|, i = 1, ..., N$
2. Augment the support set $\mathbf{\Lambda}_t = \mathbf{\Lambda}_{t-1} \cup \{\lambda_t\}$ and sub-matrix $\mathbf{D}_t = [\mathbf{D}_{t-1}\ \mathbf{d}_{\lambda_t}]$, set the λ_t column of $\mathbf{D}$ matrix to zero $\mathbf{D}(:, \lambda_t) = 0$.
3. Calculate a new estimation of support column vector $\hat{\mathbf{u}}_t = \arg\min \|\mathbf{v} - \mathbf{D}_t \mathbf{u}_t\|_2 = (\mathbf{D}_t{}^H \mathbf{D}_t)^{-1} \mathbf{D}_t{}^H \mathbf{v}$
4. Update the residual $\mathbf{r}_t = \mathbf{v} - \mathbf{D}_t \hat{\mathbf{u}}_t$
5. If $t > K$ or $\mathbf{r}_t \le \varepsilon_{th}$, then stop iteration. Otherwise, iterate from step 1., and $t = t + 1$.
3). Output $\hat{\mathbf{u}} = \hat{\mathbf{u}}_t$, $\mathbf{\Lambda} = \mathbf{\Lambda}_t$, and $\mathbf{D}_s = \mathbf{D}_t$.

$$\mathbf{f} = (\mathbf{\Lambda} - 1) * \Delta' f \tag{21}$$

$$\mathbf{Am} = abs(\hat{\mathbf{A}}) \tag{22}$$

$$\mathbf{Ph} = \mathrm{angle}(\hat{\mathbf{A}}) \tag{23}$$

When measurement noise is present, replacing (10) into (20), and the estimate is shown as

$$\hat{\mathbf{A}} = \mathbf{A} + (\mathbf{D}_S{}^H \mathbf{D}_S)^{-1} \mathbf{D}_S{}^H \mathbf{W} \tag{24}$$

If the noise is very weak, we have reason to suppose that the support recovery step can still be successfully identified. However, when the SNR is below a threshold, the support recovery is no longer deterministic and the estimation accuracy cannot be guaranteed.

D. Dynamic time-varying analysis for supraharmonics

In order to analyze the dynamic time-varying characteristics of supraharmonics, we combine the MCS-OMP algorithm with 3-D display method to display the computed supraharmonics high-resolution spectrum array in time-frequency form. Each column of the high-resolution spectral array corresponds to a time scale. Compared with 200 ms, the data block length of 0.5 ms is relatively short, so we consider that the supraharmonics are steady in each 0.5 ms observation time. Then the recovered supraharmonics spectrum array is displayed in 3-D, and the dynamic time-varying characteristics of supraharmonics components in the signal under test can be directly observed.

E. Selection of interpolation factor F

For $\delta \in (0, 0.36)$, [19] investigated the relationship between the *N*-dimensional observation vector and the *NF*-dimensional *K* sparse measurement vector in the SMV model under Gaussian distribution. The recovery probability of OMP will exceed $1 - \delta$.

$$N \ge mK \ln(NF / \delta) \tag{25}$$

where *N* is the original vector's dimension, *F* is the interpolation factor, *K* is the sparsity of the recovery vector, and *m* is a coefficient. The estimation formula of *F* is

TABLE II
PARAMETERS OF SUPRAHARMONICS IN SIMULATION SIGNAL

No.	Frequency (kHz)	Magnitude (a.u.)	Phase (rad)
1	10.2	1	0
2	21.0	1	0
3	70.6	1	0

TABLE III
COMPUTATION TIME OF THREE ALGORITHMS

Algorithm	Computation time (s)
DFT	0.036
SCS-OMP	39.867
MCS-OMP	0.401

$$F \le \frac{1}{N}\exp(N/mK) \tag{26}$$

It should be noted that the frequency resolution of the analyzed signal's spectrum couldn't be enhanced indefinitely by arbitrarily increasing the value of the interpolation factor F. The reason is that, firstly, if the interpolation factor is set too large, the condition number of the sensing matrix will be large, and the condition number reflects the stability of the matrix when it is disturbed by noise, i.e., the larger the condition number, the more unstable the matrix. Secondly, in the compressive sensing calculation, it is always desirable that the subset of any column vectors of the sensing matrix is nearly orthogonal, and if the interpolation factor F is too large, it will be difficult to meet the orthogonal condition. In summary, based on the actual needs and theoretical analysis, combined with the computation complexity and computation accuracy, the value of F is usually no more than 10.

F. Estimation of sparsity K

The purpose of the compressive sensing recovery algorithm is to map the eigenvalue column vector $\mathbf{v}$ to the support column vector $\mathbf{u}$ using the sensing matrix $\mathbf{D}$, so that there are only a small number of non-zero components and the number of non-zero components is the sparsity level of $\mathbf{u}$. The estimation of sparsity is an important iteration condition for performing the OMP algorithm. If the sparsity level estimation is not accurate, the estimation of the support set will not be accurate. In the frequency domain, if there is no spectral leakage, the signal's sparsity is equal to two times the number of supraharmonics in the analyzed signal. Some effective methods, such as Minimum Description Length (MDL) [20], and Gerschgorin Disk Estimation (GDE) [21], perform well in estimating supraharmonics components. Practice shows that in the white noise case, MDL has better performance in estimating the number of supraharmonics in signals under test, but in the situation of colored noise, the GDE criterion has a better performance.

III. SIMULATION RESULTS OF MCS-OMP ALGORITHM

A. Supraharmonics simulation model

We give the frequency, amplitude and initial phase of each supraharmonics component for simulation in TABLE II.

The sampling frequency is set to 500 kHz. We apply a 0.5 ms rectangular window to the 200 ms sampled data sequence to divide it into 400 small data blocks, and each small data block contains 250 data. All small data blocks are transformed to the frequency domain by DFT, and we obtain 400 groups of spectrums with the frequency resolution of 2 kHz. In order to improve the frequency resolution of the 400 groups of spectrums, we set the interpolation factor F to 10. The SCS-OMP algorithm in [15] and the MCS-OMP algorithm proposed in this paper are respectively used to increase the frequency resolution from the original 2 kHz to 200 Hz, and then to get supraharmonics high-resolution analysis for all 400 groups of spectrums.

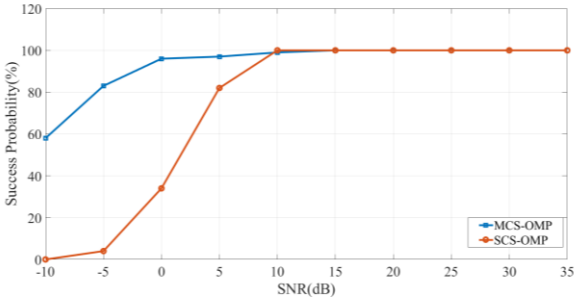

Fig. 1. Support set recovery success probability versus SNR.

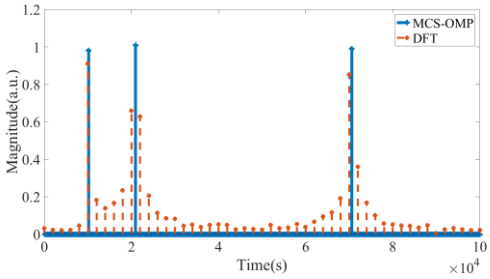

Fig. 2. Spectrum for the first data block obtained by MCS-OMP and DFT.

B. Support set recovery success probability

Adding Gaussian white noise to the supraharmonics simulation model set in TABLE II, the signal-to-noise ratio (SNR) range is set -10 to +35 dB, and the increasing step is set to 5 dB. Using the two algorithms mentioned above, we perform 100 times support set recovery under each SNR value. The number of successful recoveries of the support set is the success probability, as shown in Fig. 1.

As can be seen from Fig. 1, when the SNR is above 10 dB, the recovery success rates of the two algorithms all reach 100%. However, when the SNR is below 10 dB, the success probability of the SCS-OMP algorithm decreases significantly. The MCS-OMP algorithm still has a high recovery success probability. Even when the SNR equals 0 dB, the recovery success probability of the support set still reaches over 90%, indicating that the MCS-OMP algorithm has better robustness.

C. Comparison of computation time

In order to compare the computation time of the DFT algorithm, SCS-OMP algorithm and MCS-OMP algorithm, the SNR is set to 20 dB. The simulation software runs on Matlab2017a, and the computer configuration includes an Intel Core i5 processor, 8 gigabytes memory, and a Windows 7 64-bit operating system. We give the computation time of the three

TABLE IV
PARAMETERS OF SUPRAHARMONICS ESTIMATED BY MCS-OMP

No.	1	2	3
Frequency(kHz)	10.2	21.0	70.6
Magnitude(a.u.)	0.9998	1.0000	0.9993
Error(relative)	2×10^{-4}	0	7×10^{-4}

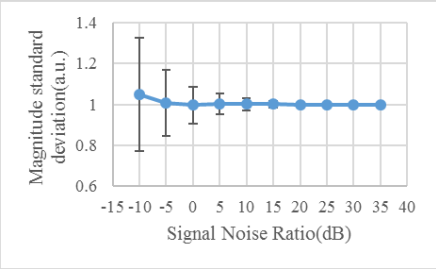

Fig. 3. Average magnitude and its standard deviation versus SNR.

algorithms in TABLE III.

We can see from TABLE III that the DFT algorithm has the shortest computation time, 0.036 s. Since SCS-OMP algorithm can only achieve supraharmonics high-resolution analysis for one original spectrum vector simultaneously, so computation time is the longest, reaching 39.867 s. The computation time of the MCS-OMP algorithm is about 0.401 s, which is about 10 times longer than that of the DFT algorithm. But, compared with the SCS-OMP, the computation time saved is about 100 times, which shows that the MCS-OMP algorithm can meet the real-time supraharmonics high-resolution measurement.

D. Comparison of computation accuracy

We use the MCS-OMP algorithm and DFT algorithm to analyze frequency and amplitudes of supraharmonics. Fig. 2 shows the spectrum obtained using the MCS-OMP algorithm and the DFT algorithm for the first data block. The SNR is set to 20 dB.

It can be seen from Fig. 2 that the spectral leakage of the DFT algorithm is very obvious at a frequency resolution of 2 kHz, while the frequency resolution of 200 Hz is improved by using the MCS-OMP algorithm, which not only eliminates the influence of spectral leakage, but also the frequency and amplitudes can be computed accurately.

We compute the frequency and amplitudes of supraharmonics by (21) and (22). Magnitude is the average of the 400 groups' data, and the error is very small. See TABLE IV for details.

With the SNR range of -10 to +35 dB in 5 dB steps, the average and standard deviation of the 400 amplitudes for supraharmonics at 10.2 kHz are shown in Fig. 3.

From Fig. 3 we can see that when the SNR is greater than 10 dB, the average value of the amplitude is closer to the setting value, and the corresponding standard deviation is smaller. In contrast, when the SNR is lower than 10 dB, the average value of the amplitude deviates from the setting value greatly, and the corresponding standard deviation is large too.

E. Dynamic analysis of supraharmonics

In order to verify the dynamic analysis performance of the algorithm proposed in this paper, we set the attenuation factors of the supraharmonics at frequencies 10.2 kHz, 21.0 kHz and 70.6 kHz to 5, 3 and 0, respectively. The interpolation factor F is set to 10 and the SNR is set to 20 dB. The 3-D spectrum obtained by the DFT algorithm and MCS-OMP algorithm, respectively, are shown in Fig. 4.

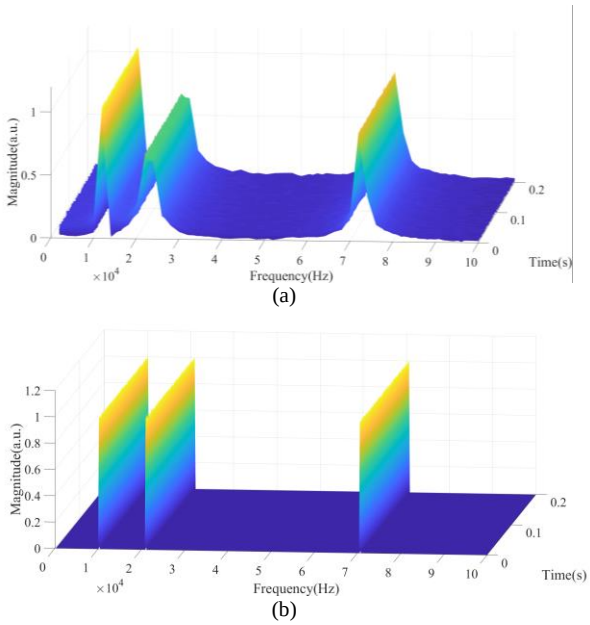

Fig. 4. 3-D spectrogram of supraharmonics. (a) Original spectrum array obtained by DFT algorithm. (b) Supraharmonics high-resolution spectrum array obtained by MCS-OMP algorithm.

It can be seen from Fig. 4 that the supraharmonics component at 10.2 kHz attenuates fast, the supraharmonics component at 21.0 kHz attenuates slowly, and the supraharmonics component at 70.6 kHz does not attenuate at all. The trend is consistent with the supraharmonics' attenuation factors set to 5, 3 and 0, respectively. At the same time, we can see from Fig. 4(a) that the spectral leakage in the frequency spectrum obtained by the DFT algorithm is relatively obvious. From Fig. 4(b), we can see that by using the MCS-OMP algorithm, we can not only realize supraharmonics high-resolution analysis, but also effectively inhibit the spectral leakage. Noise only appears at the frequency of supraharmonics. This shows that the MCS-OMP algorithm has strong anti-interference ability, the high-resolution analysis result of supraharmonics is more accurate, and the dynamic analysis result can accurately reflect the dynamic characteristics of supraharmonics.

IV. ANALYSIS OF MEASURED DATA

A. Analysis of Output Data of Wireless Electric Vehicle Charging Pile Inverter

The MCS-OMP algorithm was used to perform supraharmonics high-resolution analysis of the measured data of a wireless electric vehicle charging device. The working principle of the wireless electric vehicle charging pile is shown in Fig. 5.

The three-phase supply voltage is converted into a DC voltage by a rectifier, and then converted into an AC signal by an inverter operating at a frequency of 80 kHz and transmitted by a wireless transmitter. The wireless receiver receives the AC signal and converts it into a DC signal with a rectifier to charge

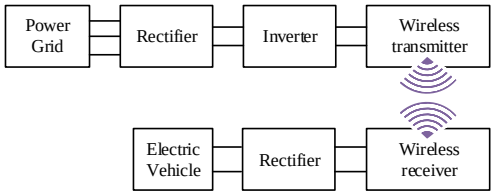

Fig. 5. Wireless electric vehicle charging pile working diagram.

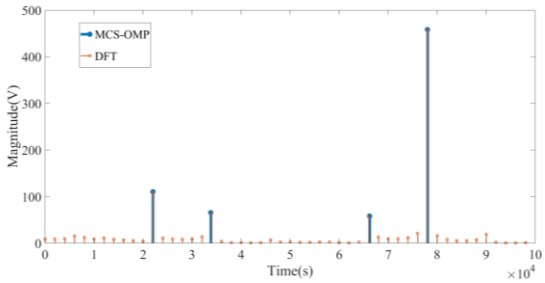

Fig. 6. Analysis results of the first data block.

the battery of the electric vehicle. Using the HIOKI MR8875 recorder and CT9692 current clamp, we recorded the voltage and current signals of the wireless transmitter input and the wireless receiver output. The sampling frequency was set to 200 kHz. Similarly, we used a Chebyshev bandpass digital filter to obtain supraharmonics in 2 to 150 kHz in 200 ms recorded data.

A rectangular window is applied to the filtered data, which is divided into 400 small data blocks of 0.5 ms and then all data blocks are transformed into 400 spectrum vectors. We compose the 400 spectrum vectors into an array, as in the original spectrum array. By using the MCS-OMP algorithm, the supraharmonics high-resolution analysis can be achieved. Sparsity is set to 8 and the interpolation factor is set to 10. Therefore, the frequency resolution of the original spectrum array can be refined to 200 Hz. Fig. 6 shows the analysis results of the first small data block of the voltage data measured at the wireless transmitter input using the MCS-OMP algorithm and DFT algorithm.

It can be clearly seen from Fig. 6 that the analysis results of the MCS-OMP algorithm and DFT algorithm are relatively consistent, while the MCS-OMP algorithm effectively overcomes the inherent spectral leakage problem of the DFT algorithm and increases the frequency resolution to 200 Hz. Four supraharmonics components were accurately detected, and the estimated parameters of the supraharmonics are shown in TABLE V.

As can be seen from Fig. 7, the frequencies and amplitudes of the four supraharmonics components remain constant within 200 ms.

B. Analysis on measured data of power supply of moisture detection device in a paper mill

An ultrasonic moisture detection device used to detect the moisture content of paper in a paper mill has caused two accidents with the control circuit board. We used a PQ-Box 200 power quality analyzer to measure the power supply of the ultrasonic moisture detection device, and the measured supply current data was calculated and analyzed using the MCS-OMP algorithm proposed in this paper. The sampling rate was set to 40.96 kHz, and the 200 ms measurement data was digitally filtered to filter out the fundamental component. Then, it was

TABLE V
PARAMETERS OF SUPRAHARMONICS ESTIMATED BY MCS-OMP

No.	Frequency(Hz)	Magnitude(V)
1	22.0k	110.15
2	30.8k	65.41
3	66.2k	57.95
4	78.0k	458.14

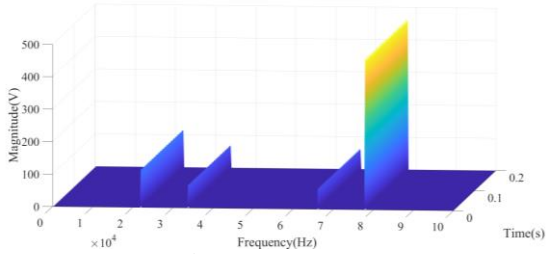

Fig. 7. Dynamic analysis of wireless electric vehicle charging pile inverter output signal.

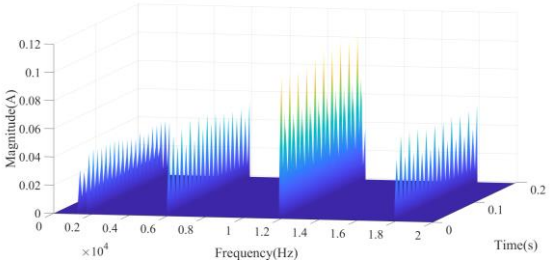

Fig. 8. 3-D spectrogram of supraharmonics in power supply of moisture detection device.

continuously divided into 40 small data blocks with a duration of 5 ms (each small data block contains 204 sampling points). The interpolation factor was set to 10, so that the frequency resolution could be refined to 20 Hz.The 3-D high-resolution spectrum of the supraharmonics is shown in Fig. 8.

From Fig. 8, we can see that in addition to the supraharmonics at 1.8 kHz, the measured signal also contains supraharmonics at 6 kHz, 12 kHz and 18 kHz, which are generated at the switching frequency and its integral multiple frequency during the power electronic switching device operation. These supraharmonics clearly fluctuate with time, indicating that the supraharmonics have time-varying characteristics.

V. CONCLUSION

In this paper, we propose and establish a new supraharmonics high-resolution measurement algorithm, called MCS-OMP algorithm. Specifically, by introducing an interpolation factor, and based on a spectrum array of multiple DFT coefficient vectors and a Dirichlet kernel matrix, we construct a MMV compressive sensing model. Because of the jointly sparse features of the high-resolution spectrum array, we convert the MMV compressive sensing model into a SMV compressive sensing model, and then use the OMP algorithm to solve the support set, which is also the support set of the high-resolution spectrum array. According to the support set, the column vector of the sensing matrix is extracted to form the sub-matrix. Finally, we use the least squares algorithm to achieve the supraharmonics high-resolution analysis of the original

spectrum array simultaneously. This algorithm does not have the inherent defects of the observation time and frequency resolution of the DFT algorithm. Without increasing the observation time of the measured data, it breaks through the limitation of the Shannon's sampling theorem, which can not only achieve accurate positioning of the supraharmonics frequency in the measured signal, but can also compute the amplitudes of supraharmonics accurately. The new algorithm has a high computation speed and a good anti-interference ability, which can meet the requirements of real-time high-resolution measurement of supraharmonics. The above theoretical analysis conclusions are confirmed by simulation analysis and verification of the measured data.

By combining the MCS-OMP algorithm with the 3-D time-frequency display method, the new measurement algorithm can not only display the spectrum of supraharmonics with high-resolution, but also show clearly the dynamic characteristics of each supraharmonics component with time. It can be seen that the MCS-OMP algorithm proposed in this paper can provide a useful measurement algorithm for in-depth study of the propagation characteristics, interaction mechanism, emission limit and inhibition of supraharmonics.

REFERENCES

[1] A. A. Girgis, M. C. Clapp, E. B. Makram, et al., "Measurement and characterization of harmonic and high frequency distortion for a large industrial load," *IEEE Trans. Power Delivery*, vol. 5, no. 1, pp. 427–434, 1990.

[2] S. K. Rönnberg, M. H. J. Bollen, H. Amaris, et al, "On waveform distortion in the frequency range of 2 kHz–150 kHz—Review and research challenges," *Electric Power Systems Research*, vol. 150, pp. 1–10, 2017.

[3] M. Klatt, J. Meyer, P. Schegner, et. al., "Emission levels above 2 kHz-laboratory results and survey measurements in public low voltage grids," in *22th CIRED*, Stockholm, Sweden, 2013, pp. 1168–1168.

[4] A. Emanuel, A. McEachern, "Electric Power Definitions: a Debate," in *IEEE Power and Energy Society General Meeting*, Vancouver, BC, Canada, 2013, pp. 21–25.

[5] SC 205A, "Study report on electromagnetic interference between electrical equipment/systems in the frequency range below 150 kHz," CENELEC, Tech. Rep. CLC/TR 50627, Nov. 2015.

[6] J. Meyer, M. Klatt, R. Stiegler, "Supraharmonics (2 to 150 kHz) in low voltage networks," in *24th CIRED*, Glasgow, United Kingdom, 2017, pp. 1–30.

[7] J. Meyer, M. Bollen, H. Amaris, et al., "Future work on harmonics-some expert opinions Part II-supraharmonics, standards and measurements," in *16th ICHQP*, Bucharest, Romania, 2014, pp. 909–913.

[8] A. Larsson, M. Bollen, "Towards a standardized measurement method for voltage and current distortion in the frequency range 2 to 150 kHz," in 22nd *CIRED*, Stockholm, Sweden, 2013, pp. 1–4.

[9] R. Schmidt, "Multiple emitter location and signal parameter estimation," *IEEE Trans. Antennas and Propagation*, vol. 34, no. 3, pp. 276–280, 1986.

[10] R. Roy, T. Kailath, "ESPRIT-estimation of signal parameters via rotational invariance techniques," *IEEE Trans. Acoustics, Speech, and Signal processing*, vol. 37, no. 7, pp.984–995, 1989.

[11] E. J. Candès, J. Romberg, T. Tao, "Robust uncertainty principles: Exact signal reconstruction from highly incomplete frequency information," *IEEE Trans. Information Theory*, vol. 52, no. 2, pp.489–509, 2006.

[12] E. J. Candès, J. Romberg, T. Tao, "Stable signal recovery from incomplete and inaccurate measurements," *Communications on pure and applied mathematics*, vol. 59, no. 8, pp.1207–1223, 2006.

[13] D. L. Donoho, "Compressed sensing," *IEEE Trans. information theory*, vol. 52, no. 4, pp.1289–1306, 2006.

[14] M. Bertocco, G. Frigo, C. Narduzzi, et al., "Resolution enhancement by compressive sensing in power quality and phasor measurement," *IEEE Trans. Instrumentation and Measurement*, vol. 63, no. 10, pp. 2358–2367, 2014.

[15] S. Zhuang, W. Zhao, Q. Wang, S. Huang, "A New Measurement Method for Supraharmonics in 2-150 kHz," *Proceedings of 2018 Conference on Precision Electromagnetic Measurements*, pp. 1–2, 2018.

[16] J. A. Tropp, A. C. Gilbert, "Signal recovery from random measurements via orthogonal matching pursuit," *IEEE Trans. Information Theory*, vol. 53, no. 12, pp. 4655–4666, 2007.

[17] G. Frigo, C. Narduzzi, "Characterization of a compressive sensing preprocessor for vector signal analysis," *IEEE Trans. Instrumentation and Measurement*, vol. 65, no. 6, pp. 1319–1330, 2016.

[18] M. Mishali, Y. C. Eldar, "Reduce and boost: Recovering arbitrary sets of jointly sparse vectors," *IEEE Trans Signal Processing*, vol. 56, no. 10, pp. 4692–4702, 2008.

[19] E. J. CANDÈS, M. B. WAKIN, "An introduction to compressive sampling," *IEEE Signal Processing Magazine*, vol. 25, no. 2, pp. 21–30, 2008.

[20] J. Rissanen, "A Universal prior for integers and estimation by minimum description length", *The Annals of statistics*, pp. 416–431, 1983.

[21] H. T. Wu, J. F. Yang, F. K. Chen, "Source number estimator using gerschgorin disks," in *ICASSP-94*. pp. IV/261–IV/264, 1994.

Shuangyong Zhuang received the B.S. degree from Measurement and Instrument, Xiamen University, Xiamen, China, in 2000, and M.S. degree in Communication and Information System from Sichuan University, Chengdu, China, in 2007.

Now he is a Ph.D. candidate in the Department of Electrical Engineering, Tsinghua University, Beijing, China. His current research interests include modern power quality analysis.

Wei Zhao received the B.S. degree in electrical engineering from Tsinghua University in 1982 and Ph.D. degree in electrical engineering from Moscow Energy Institute, Moscow, Russia, in 1991.

Now, he is a professor in the Department of Electrical Engineering, Tsinghua University, Beijing, China. His current research interests include electromagnetic measurement and instrumentation.

Ren Wang received the B.S. degree in 2012 from the Department of Electrical Engineering, Shanghai University of Electrical Power, Shanghai, China. He is currently pursuing the Ph.D. degree in the Electrical Engineering Department, Tsinghua University, Beijing, China.

His research interests include compressive sensing, machine learning, signal detection and estimation.